

Calculation of Particle Emission Rates for Nucleon-Induced Reactions with non-Equidistance Spacing Model Dependence

Ahmed Abdul-Razzaq Selman

IT Unit, College of Science, University of Baghdad, Baghdad-Iraq

E-mail: ahmed@aaselman.com

Abstract

Nuclear emission rates for nucleon-induced reactions are theoretically calculated based on the one-component exciton model that uses state density with non-Equidistance Spacing Model (non-ESM). Fair comparison is made from different state density values that assumed various degrees of approximation formulae, beside the zeroth-order formula corresponding to the ESM. Calculations were made for ^{96}Mo nucleus subjected to (N,N) reaction at $E_{\text{max}}=50$ MeV. The results showed that the non-ESM treatment for the state density will significantly improve the emission rates calculated for various exciton configurations. Three terms might suffice a proper calculation, but the results kept changing even for ten terms. However, five terms is found to give the most appropriate conditions for calculation time and accuracy.

Keywords

Particle Emission Rates
Nucleon-Induced Reactions

Article info

Received: Mar. 2010

Accepted: Apr. 2010

Published: Jan. 2011

حساب معدلات انبعاث الجسيمة من التفاعلات المحفزة بالنويات المعتمدة على النموذج الغير متساوي البعد

أحمد عبد الرزاق سلمان

وحدة تكنولوجيا المعلومات – كلية العلوم – جامعة بغداد

الخلاصة

حُسبت معدلات الانبعاث النووية من التفاعلات المحفزة بالنوية نظريا بالاعتماد على نموذج الجسيمة المهيجة لنظام مكون من نوع واحد من الجسيمات وبافتراض التوزيع الغير متساوي البعد في حسابات كثافة الحالات النووية. أُجريت مقارنات كافية لقيم كثافة المستويات المختلفة على افتراض عدد من المعادلات التقريبية، بالإضافة إلى المعادلة الصفرية التي تمثل حالة التوزيع المتساوي. الحسابات أُجريت لنواة ^{96}Mo خاضعة لتفاعل (نوية،نوية) عند طاقة عظمى 50 مليون إلكترون فولط. بينت النتائج أن تأثير التوزيع الغير متساوي البعد في حسابات كثافة الحالات النووية سيحسن وبصورة مميزة من معدلات الانبعاث النووية ولمختلف التوزيعات. لوحظ أن ثلاثة حدود في حساب كثافة الحالات قد يفي بدقة مناسبة، لكن النتائج استمرت بالتغير البسيط ولحد عشرة حدود. وُجد أن خمسة حدود تعتبر الحالة الملائمة والتي تجمع بين دقة الحسابات وزمن الحساب.

<i>List of symbols used in this work.</i>	
A	Mass number of the target nucleus
$A_{p,h}$	Pauli blocking energy
B	Binding energy of the emitted nucleon
C_{ak} and C_{bj}	Numerical coefficients
E	Excitation energy
F	Fermi energy of the target nucleus
$T(p,h,n,E)$	Equilibration time for the exciton state described by (p,h,n,E)
$W(p,h,n,E)$	Particle emission rate from a state defined by (p,h,n,E)
$\Theta(x - x_0)$	The Heaviside step function
d	Energy spacing in the ESM approach
g_o, g, g_p and g_h	Single-particle level density (s.p.l.d.) respectively for the ground state, the average excited states, particle and hole
$\alpha_{p,h}$	Correction term due to Pauli principle
ε	Exciton energy
$\omega(p, h, E)$	State density of the system for p particles, h holes and excitation energy E . A superscript (E) stands for Ericson's formula, and (W) for Williams'
$\varepsilon^{(p)}$ and $\varepsilon^{(h)}$	Single particle and hole excitation energies
n, p, h	Exciton, particle and hole numbers; $n=p+h$
r_o, m	Nucleon classical radius and its effective rest mass
s_b	Spin of the emitted particle
μ_b	Reduced mass of the (emitted particle-residual nucleus) system
$\sigma_r(\varepsilon)$	Inverse-reaction cross-section

Introduction

State density has a major importance in the calculations of the nuclear exciton model. This model, first suggested by Griffin [1] as a semi-classical model, describes nuclear reaction between incident projectile and target nucleus as a series of exciton (particle and hole) creation, a process responsible of distributing the incident energy among nuclear constituents thus gradually exciting the nucleus. The final state in this process is the equilibrium state, where the compound nucleus is created. During exciton development, nuclear emission might take place. The mechanism of exciton creation

explains energy sharing and nucleon emission, which is expressed by the ratio between (partial) state density of residual states to that of the initially excited state. This model was rapidly developed, over the past decades and it is represented in the present day as a family of models that aim to explain nuclear reactions responsible of continuum emission [2-8]. Such emission, the Preequilibrium Emission (PE), well describes nuclear reactions of various projectile-ejectile types at intermediate energies (~10-150 MeV). During the development of the exciton model, there had been many important corrections added to state density calculations in order to improve the overall results of the model. Such corrections included Pauli principle [9], pairing [10-11], surface and finite-well depth corrections [12,13], shell effects [14], and other corrections [15-18].

In this paper, the state density calculated from the non-ESM system are applied to the emission rate for ^{96}Mo , suffering from (N,N) reaction at maximum energy 50 MeV. This is compared with various approximation terms as well as with emission rates calculated from the ESM approach. Detailed discussions are given for the effects of approximation terms, exciton configuration and excitation energy. Beside this, an emission rate calculation has been performed for the conditions of bounded and unbounded particles states.

State Density of Nuclear Exciton States

A key parameter in state density description is the single-particle level density (s.p.l.d.), g . In general, two approaches are available to describe s.p.l.d. dependence on the particle and hole energy levels, ε_p and ε_h from Fermi surface F . The first approach assumes that g is constant of energy for all particle-hole states, and is called the Equidistance Spacing Model (ESM). The second approach represents the more realistic one where an attempt is made to describe the

dependence of g on ε_p and ε_h , and is called the (non-ESM). There are two types of the exciton model, the one-component model which assumes that protons and neutrons are indistinguishable particles, with total exciton number being $n=p+h$; and the two-component model which describes nucleons separately assuming proton particles p_π , proton holes h_π , and neutron particles and holes p_ν and h_ν , respectively, and $n = p_\pi + h_\pi + p_\nu + h_\nu$. In the ESM approach, the s.p.l.d. assumes the existence of an average energy spacing d between adjacent levels then,

$$g = \frac{A}{d}, \tag{1}$$

where the value of d varies from (8-25) MeV, but is usually taken from (10-15) MeV. Formula (1) is typically used for a mass number $A \geq 40$ and excitation energy $E \geq 15$ MeV [15].

In the one-component, the s.p.l.d. for particle and holes is described as [19]

$$g_p(\varepsilon_p) = g_o \sqrt{\frac{F + \varepsilon_p}{F}} \tag{2-a}$$

$$g_h(\varepsilon_h) = g_o \sqrt{\frac{F - \varepsilon_h}{F}} \tag{2-b}$$

$$\omega(p, h, E) = \frac{1}{p!h!} \int_0^\infty d\varepsilon_1^{(p)} g_p(\varepsilon_1^{(p)}) \int_0^\infty d\varepsilon_2^{(p)} g_p(\varepsilon_2^{(p)}) \dots \int_0^\infty d\varepsilon_p^{(p)} g_p(\varepsilon_p^{(p)}) \times \int_0^\infty d\varepsilon_1^{(h)} g_h(\varepsilon_1^{(h)}) \int_0^\infty d\varepsilon_2^{(h)} g_h(\varepsilon_2^{(h)}) \dots \int_0^\infty d\varepsilon_h^{(h)} g_h(\varepsilon_h^{(h)}) \delta(E - \sum_{\lambda=1}^p \varepsilon_\lambda^{(p)} - \sum_{j=1}^h \varepsilon_j^{(h)}), \tag{3}$$

where δ is Dirac delta function which is given in its integral form,

$$\delta(E - \sum_{\lambda=1}^p \varepsilon_\lambda - \sum_{j=1}^h \varepsilon_j) = \frac{1}{2\pi} \int_{-\infty}^{+\infty} dk \exp \left[ik \left(E - \sum_{\lambda=1}^p \varepsilon_\lambda - \sum_{j=1}^h \varepsilon_j \right) \right]. \tag{4}$$

In the ESM approach, one means that $g(\varepsilon) = g_o$, then eq.(3) reduces to the simplest state density formula due to Ericson [21],

$$\omega^E(p, h, E) = \frac{g^n E^{n-1}}{p!h!(n-1)!} \tag{5}$$

if Pauli exclusion principle was introduced to eq.(5), then Williams' formula [9] will be obtained,

$$\omega^W(p, h, E) = \frac{g^n (E - A_{p,h})^{n-1}}{p!h!(n-1)!} \times \Theta(E - \alpha_{p,h}) \tag{6}$$

where an assumption is made that $g_p = g_h = g$. In eq.(6), Pauli term is given as,

$$A_{p,h} = \frac{p(p+1) + h(h-3)}{4g} \tag{7}$$

and $\Theta(E - \alpha_{p,h})$ is the Heaviside step function defined as,

$$\Theta(E - \alpha_{p,h}) = \begin{cases} 0 & E - \alpha_{p,h} \leq 0 \\ 1 & E - \alpha_{p,h} > 0 \end{cases} \tag{8}$$

and the correction term $\alpha_{p,h}$ is given as [9],

$$\alpha_{p,h} = \frac{p(p+1) + h(h-1)}{2g}. \tag{9}$$

In non-ESM system, it was shown [20] that the simplest but complete solution is,

$$\omega^{non-ESM}(p, h, E) = \frac{(-1)^n g_o^n}{2^{n-1} \pi^{n/2} p! h!} \frac{\widehat{\Xi} E^{N-1}}{F^{N-n} (N-1)!}, \tag{10}$$

where

$$\widehat{\Xi} = \sum_{a_1=0}^{\infty} \sum_{a_2=0}^{\infty} \dots \sum_{a_p=0}^{\infty} (-1)^{a_1+a_2+\dots+a_p} \sum_{b_1=0}^{\infty} \sum_{b_2=0}^{\infty} \dots \sum_{b_h=0}^{\infty} \prod_{k=1}^p C_{a_k} \prod_{j=1}^h C_{b_j}, \tag{11-a}$$

$$N = n + a_1 + a_2 + \dots + a_p + b_1 + b_2 + \dots + b_h = n + \sum_{i=1}^p a_i + \sum_{j=1}^h b_j, \tag{11-b}$$

$$\left. \begin{aligned} C_{a_k} &= \left(a_k - \frac{3}{2} \right)! \\ C_{b_j} &= \left(b_j - \frac{3}{2} \right)! \end{aligned} \right\}, \tag{11-c}$$

where the indices a_k and b_j in eq.(11) describe the degree of accuracy for the system. It can be easily shown that the zeroth-order degree of eq.(10) will lead to Ericson's formula, eq.(5). When taking Pauli correction, eq.(10) will be given as [20],

$$\omega^{non-ESM \text{ with Pauli}}(p, h, E) = \frac{g_o^n}{2^n \pi^{n/2} p! h!} \frac{\widehat{\Xi} (E - A(p, h))^{N-1}}{F^{N-n} (N-1)!}. \tag{12}$$

Earlier attempts [19,22] studied the s.p.l.d. dependence on energy for the first three terms. Thus, our earlier treatment [20] gives the general treatment for state density calculations. It is important to remember here again that eq.(10) takes no restrictions on B and F yet, thus it still represents an approximation.

In the exciton model formulation, particle emission rate of a particle of type b due to nuclear reaction to the continuum is given by the relation [8]

$$W_b(p, h, n, E) = \frac{(2s_b + 1)}{\pi^2 \hbar^3} \times \mu_b \varepsilon \sigma_r(\varepsilon) \frac{\omega(p-1, h, n-1, U)}{\omega(p, h, n, E)} \tag{13}$$

where $\sigma_r(\varepsilon)$ is the inverse-reaction cross-section and it can be calculated from the systematics found in PRECO-2006 manual [23]. Thus, the emission spectrum of a particle of type b will be calculated from [8],

$$\left(\frac{d\sigma}{d\varepsilon} \right)_b = \sum_n W_b(p, h, n, E) T(p, h, n, E), \tag{14}$$

where $T(p, h, n, E)$ is the equilibration time calculated from the solving the master equation of the system and integrating the resulting occupation probabilities over time. Equilibration time calculation depends on the internal transition rates of between exciton states and the latter also depends on the state density to a high degree. For details of equilibration time and master equation solution methods see Ref. [20, 24, 25]. The importance of the state density in the exciton model calculations can be seen clearly from the above formulae.

Calculation Codes

A library of MATLAB codes were written to calculate the emission rates based on various state density formulae. All calculation were performed for one-component, for nucleon reaction and emission only. Most calculations aimed to find the numerical result of eq.(13) where most comparisons are made.

The input parameters used in this work are listed in Table (1) for two general calculation modes, those with $F=40$ and $B=10$ MeV (the bounded particle mode) and $F=100$ MeV, $B=0$ MeV (the unbounded particle mode). These modes are chosen to explain the effects of B and F on the calculations. All other input parameters were the same, and those are: $A=96$, $Z=42$, $d=13$ MeV, and $g_0=A/d\text{MeV}^{-1}$.

Results and Discussions

As seen from eq.(13), the state density enters in the emission rates by the form of the ratio between state density of residual nucleus $\omega(p-1, h, n-1, U)$ to that of the excited one $\omega(p, h, n, E)$. This ratio is found from the exciton configuration of $(p, h)=(1,1)$, $(2,1)$, $(2,2)$ and $(3,2)$ calculated for the ESM system.

Table (1). Input parameters of the present work.

Input parameter	Bounded particle mode	Unbounded particle mode
F	40 MeV	140 MeV
B	10 MeV	0 MeV
E_{max}	50 MeV	50 MeV
(p, h)	(1,1), (2,1), (2,2), (3,2)	(1,1), (2,1), (2,2), (3,2)
Calculation terms	1, 2, 3, 5, 10	3, 5

Corresponding configurations for the residual nucleus in this case are: $(p, h)=(0,1)$, $(1,1)$, $(1,2)$ and $(2,2)$, respectively, since we assumed nucleon emission only and the maximum $n=5$. This ratio is the only parameter changing during emission rate calculations since all the

other parameters of eq.(13), namely, $\frac{(2s_b + 1)}{\pi^2 \hbar^3} \mu_b \varepsilon \sigma_r(\varepsilon)$, remain the same

for all the cases under study. Because of its importance in the exciton model, the calculations and comparisons made in this paper are for the emission rates, rather than the ratio between state densities only.

In Figure (1-a), a comparison is made for the calculated emission rates for ^{96}Mo nucleus from (N,N) reaction at 50 MeV, assuming Ericson's formula for the ESM system, eq.(5), and the simple non-ESM formula eq.(10). The assumed number of terms was set to (5) in the non-ESM case. The difference between the configuration $(p, h)=(1,1)$ is quite obvious, where in the ESM case a smooth variation occurred in the entire calculated range, while in the non-ESM system the calculated rate started at energies about 10 MeV. This is explained due to the effect of the exciton configuration in the non-ESM calculations, where at low energies a negative (non-physical) value of the non-ESM state density are found, which is set to zero in the code. At $(p=1)$ in the excited nucleus, the $(p-1)$ in the residual nucleus will return zero value and the exciton configuration will read $(0, h)$, thus all summations of p in the operator $\hat{\Xi}$ of eq.(10) will be not contribute in the calculation leaving the first few terms with negative output. From the shape of eq.(10), one may interpret such a result for any total energy E larger than F . This clearly indicates that the application of this formula at such energies requires more caution. It is important here to mention that in earlier calculations [20], this was not clearly found since no practical calculations were made to investigate the effects of the non-ESM state density on nucleon emission rates. The same calculation was repeated for the unbounded conditions -Table (2)- and the result is shown in Figure (1-b). The results of (1,1) are now in a better accordance with other configuration results. The end of lines in Figure (1-a) occurred at $\varepsilon \sim 40$ MeV, which is due to the effect of

B. The code EMNUR2 loops the value of ε from (0 to $E_{\max}-B$).

Aside the case of (1,1), all other configurations share the same behavior, where in general the non-ESM emission results (with bold lines) are less than those due to the ESM. Earlier study [20] showed that the values of the state density in the non-ESM system are less than the ESM. Thus, it is clear now that both the *ratio between state densities* and the *individual values* are both less in the non-ESM, even though the present formalism still approximate.

In Figure (1-c), the same comparison is made when calculating the non-ESM for 10 terms. The general observation in all

these figures is that, as the exciton configuration develops the emission rates peaks to higher values at low energies and drop faster at higher energies. This is seen in all the present results. The only exception is the case with configuration (1,1) again, where the behavior indicates a saturation limit. In fact, this case is clearly seen from comparison of the ESM cases only for both Ericson and Williams' formulae, as given in Figure (1-d). Also it is noticed that the differences between both types of formulae are small at such reaction energy (0-50 MeV). The non-ESM comparison is given in Figure (1-e) for the same configurations. Comparing both these figures also indicates the amount of correction added when using the non-ESM treatment.

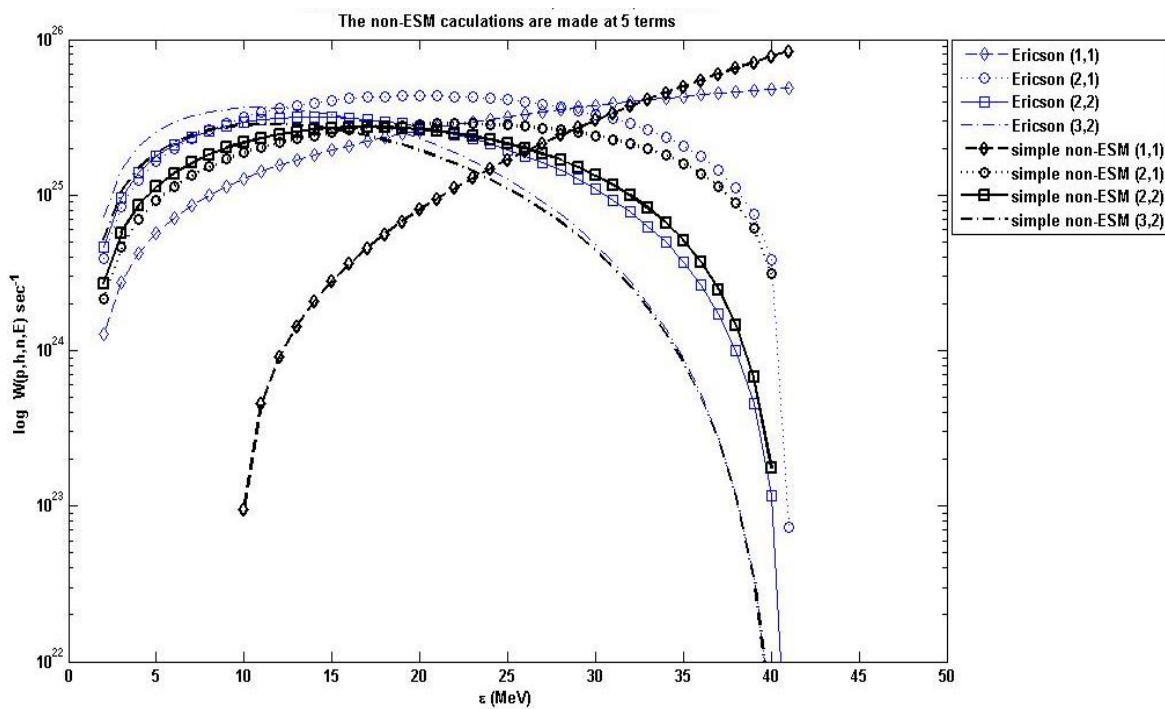


Figure (1-a). A comparison between emission rates calculated from Ericson's formula and the simplest non-ESM formula for ^{96}Mo target at 50 MeV, for various configurations. Bounded conditions are used.

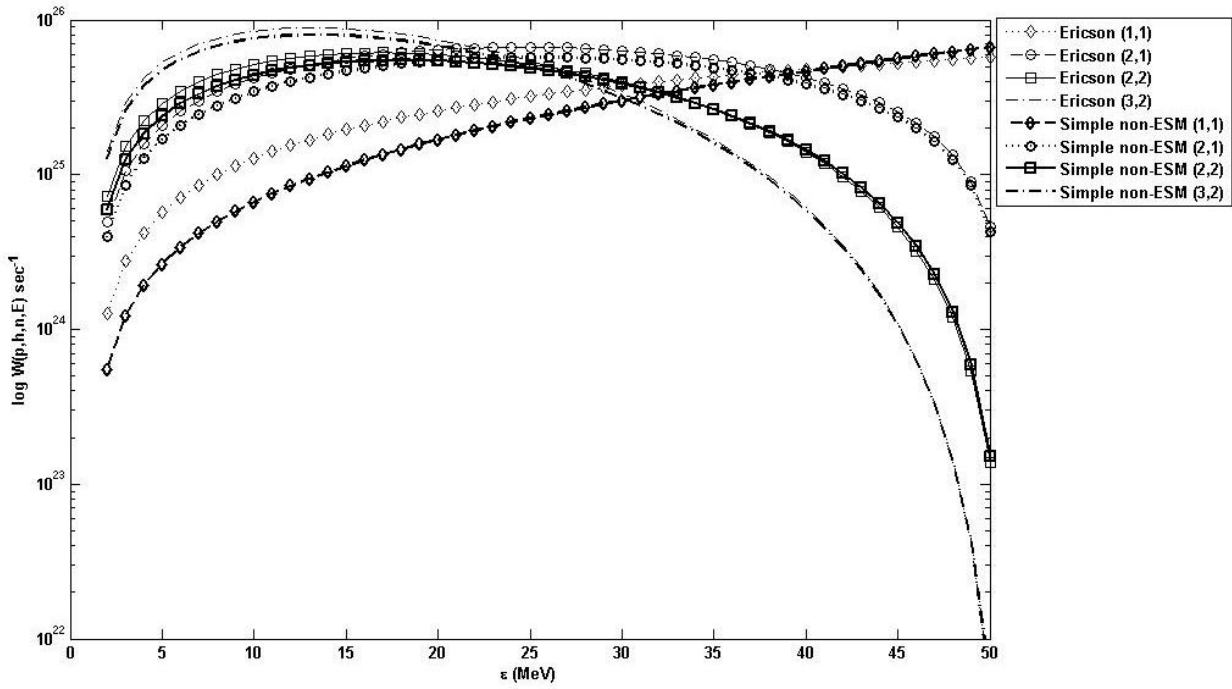


Figure (1-b). The same as Figure (1-a) for unbounded conditions.

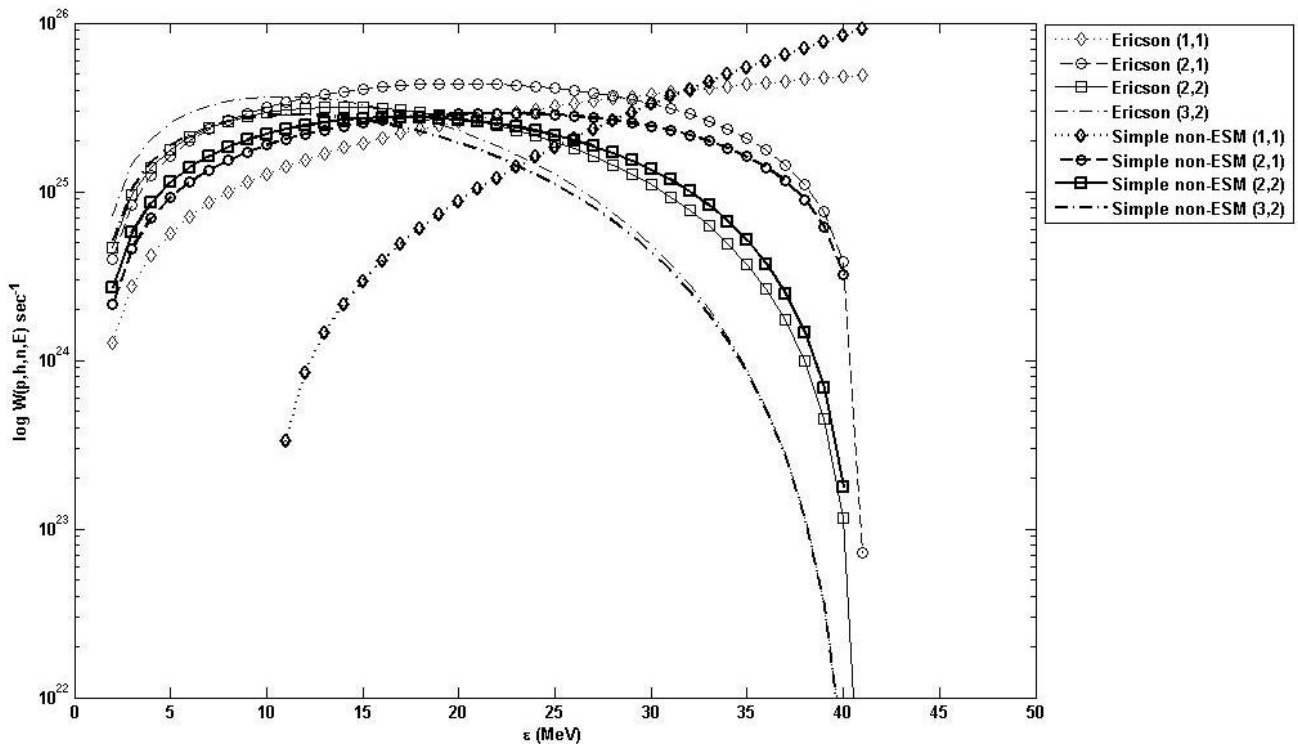


Figure (1-c). The same as Figure (1-a) with 10 terms of calculation for bounded conditions.

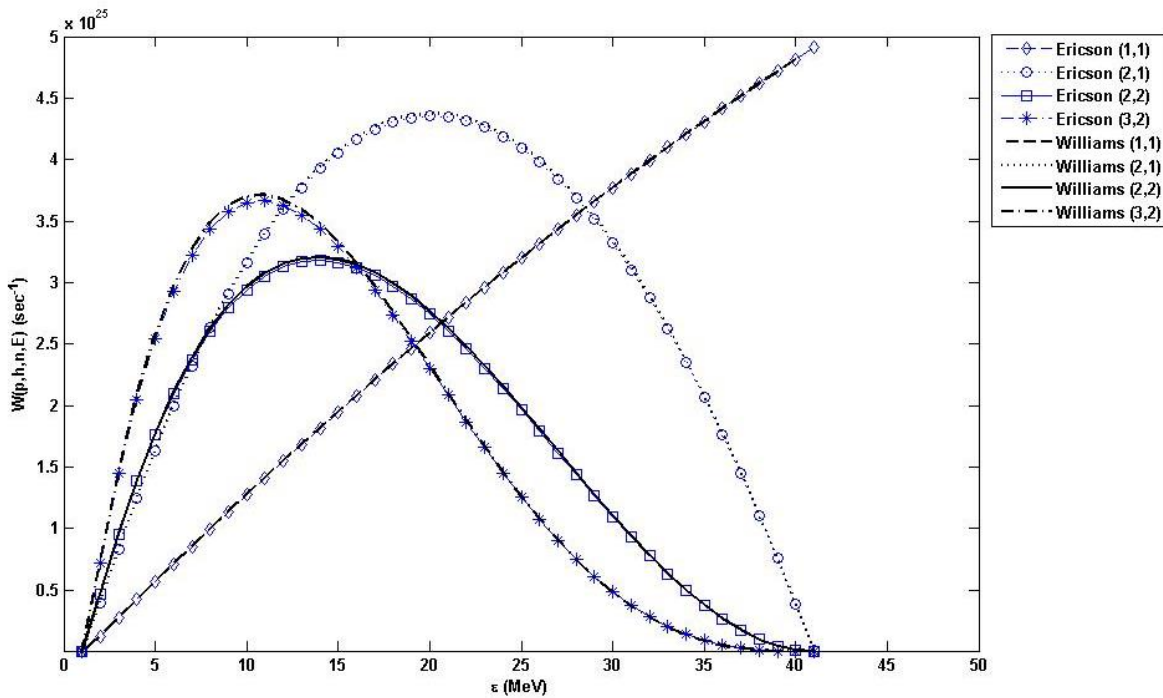


Figure (1-d). A comparison between emission rates calculated from Ericson's and Williams' formulae in the ESM system, for ^{96}Mo target at 50 MeV and for various configurations. Bounded conditions are used.

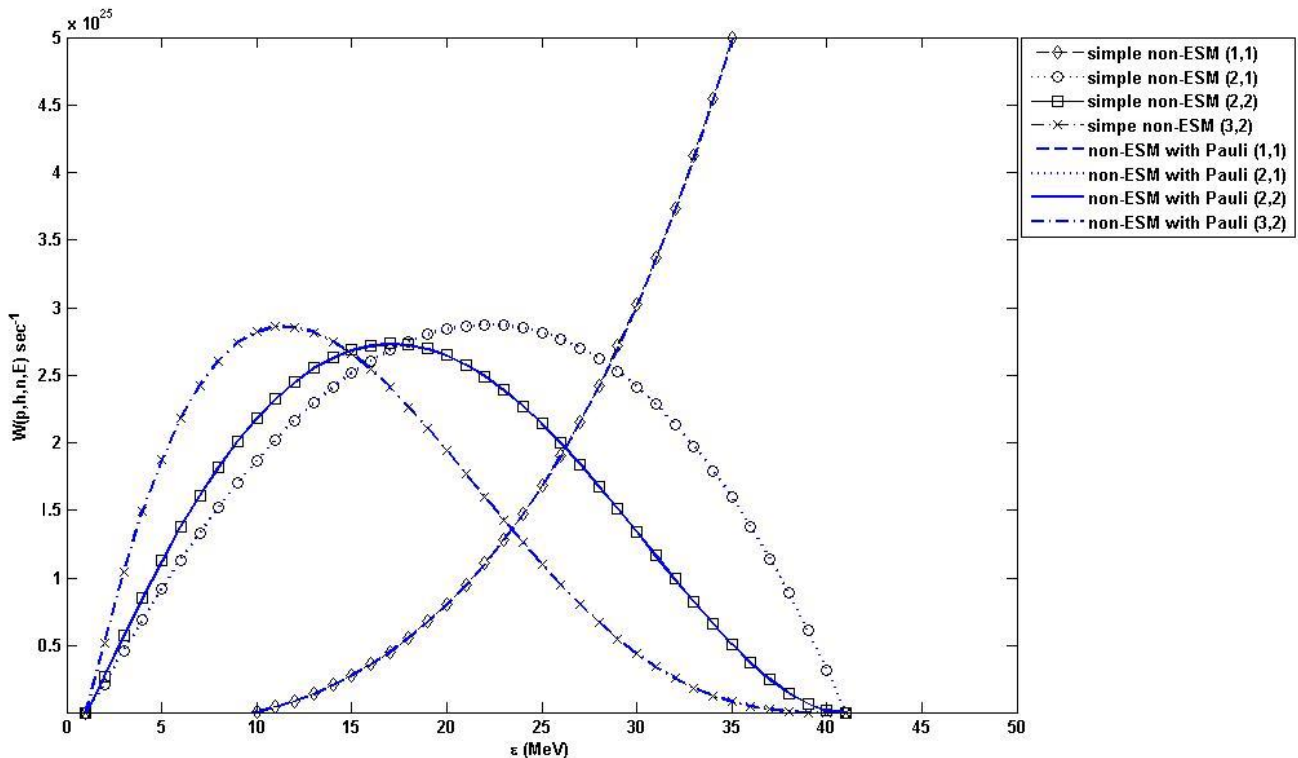


Figure (1-e). A comparison between emission rates calculated from simple non-ESM and the non-ESM with Pauli correction formulae, for ^{96}Mo target at 50 MeV and for various configurations. Only 5 terms are used with the bounded conditions.

A similar behavior is found when calculating emission rates from Williams'

formula (6) and the non-ESM with Pauli correction formula (12), as shown in Figure

(2-a), for the bounded particle conditions. Figure (2-b) shows a comparison for the above results to see the effects of calculation terms more clearly for $(p, h)=(1,1)$. From Figure (2-b), the important observation is that increasing the number of terms reduces the emission rates at the same emission energy. This indicates that the ratio of the state densities is reduced with increasing the number of terms. The values shown in this example also signifies the differences of emission rates between ESM and non-ESM emission rates when plotting with linear axis of $W(p,h,n,E)$. Similar comparisons are made in Figures (2-c) and (2-d) for exciton configurations $(p, h)=(2, 2)$ and $(3, 2)$, respectively.

Another comparison is made with the summation of the emission rates for different systems and terms, where the differences are reasonably large and obvious. This is made in Figure (3) where all the used calculations are joined by means of their sum values, for bounded particle condition. First, it can be seen that the calculations with only one term lays

between the zeroth-order approximation, the ESM, and the non-ESM system. Using two terms greatly modifies the calculation, while three terms of calculation points out the characteristic of the non-ESM treatment significantly. When calculating with five terms, the behavior continues to change and reaches almost the saturation limit, there is only some although inconsiderable change from this case and the ten terms case. Taking this result with the results of the run time of the code -Table (3)- under consideration, one reaches that five terms represent a practical choice for similar calculations.

One last comparison is made in Figure (4) between emission rates calculated for one-component with both ESM and non-ESM systems, and the two-component ESM system for configurations $(p,h)=(2,1)$ and $(3,2)$ in the one-component, and for $(p_\pi, h_\pi, p_\nu, h_\nu) = (2,1,0,0)$ and $(3,2,0,0)$ for the two-component system.

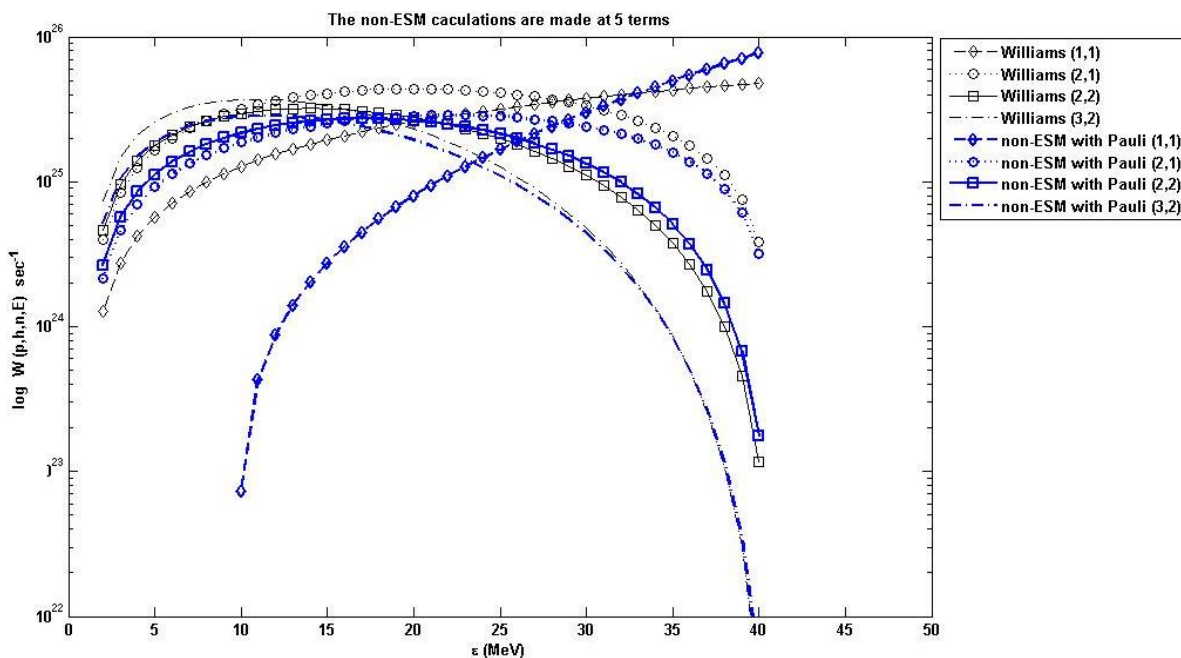


Figure (2-a). A comparison between emission rates calculated from Williams' formula and the non-ESM formula with Pauli correction for ^{96}Mo target at 50 MeV, for various configurations. Bounded conditions are used.

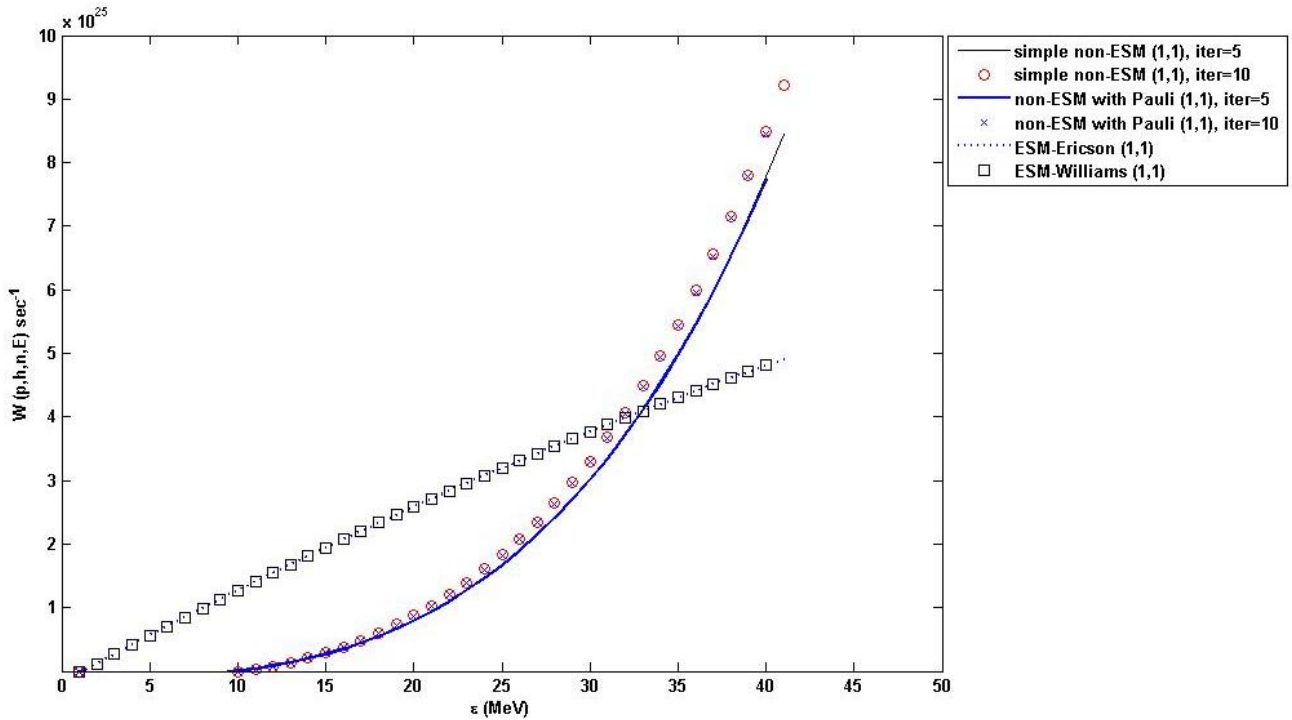


Figure (2-b). A comparison between emission rates calculated from Ericson's and Williams' formulae, with the corresponding non-ESM formulae with 5 and 10 terms of calculations, for configuration (1,1). This example is for ⁹⁶Mo target at 50 MeV, for various configurations. Bounded conditions are used.

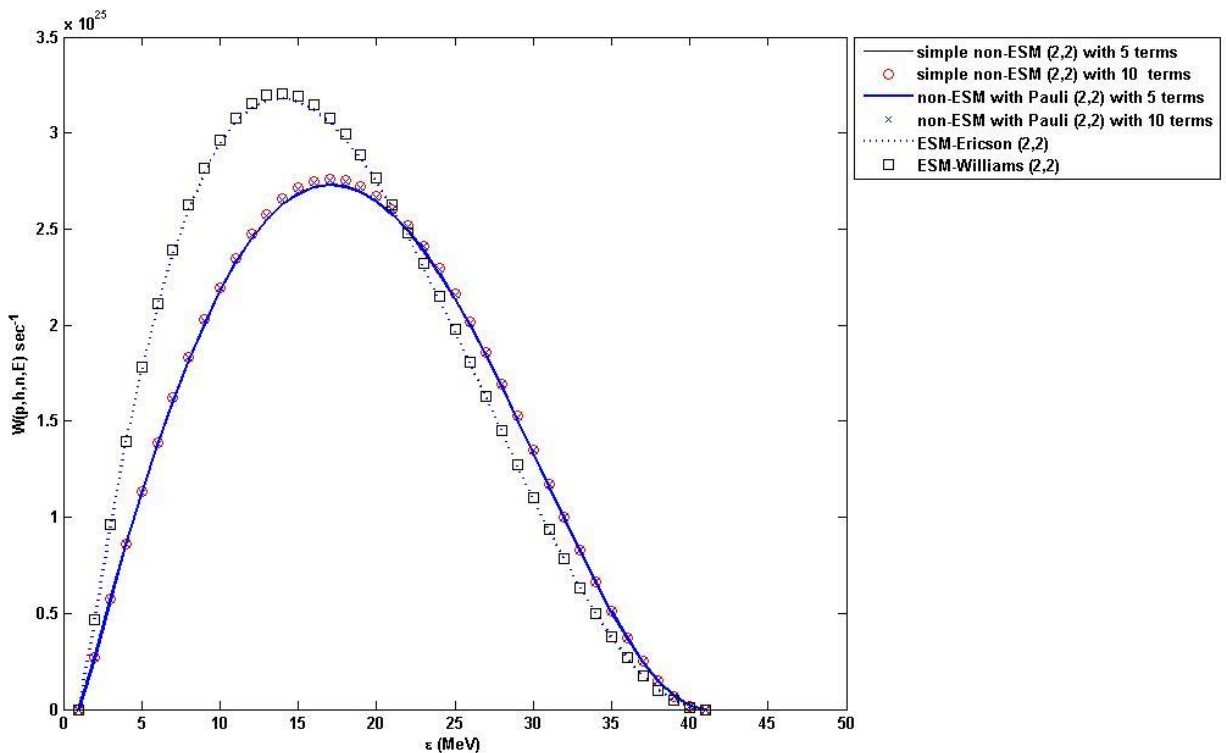


Figure (2-c). The same as Figure (2-b) for configuration (2,2).

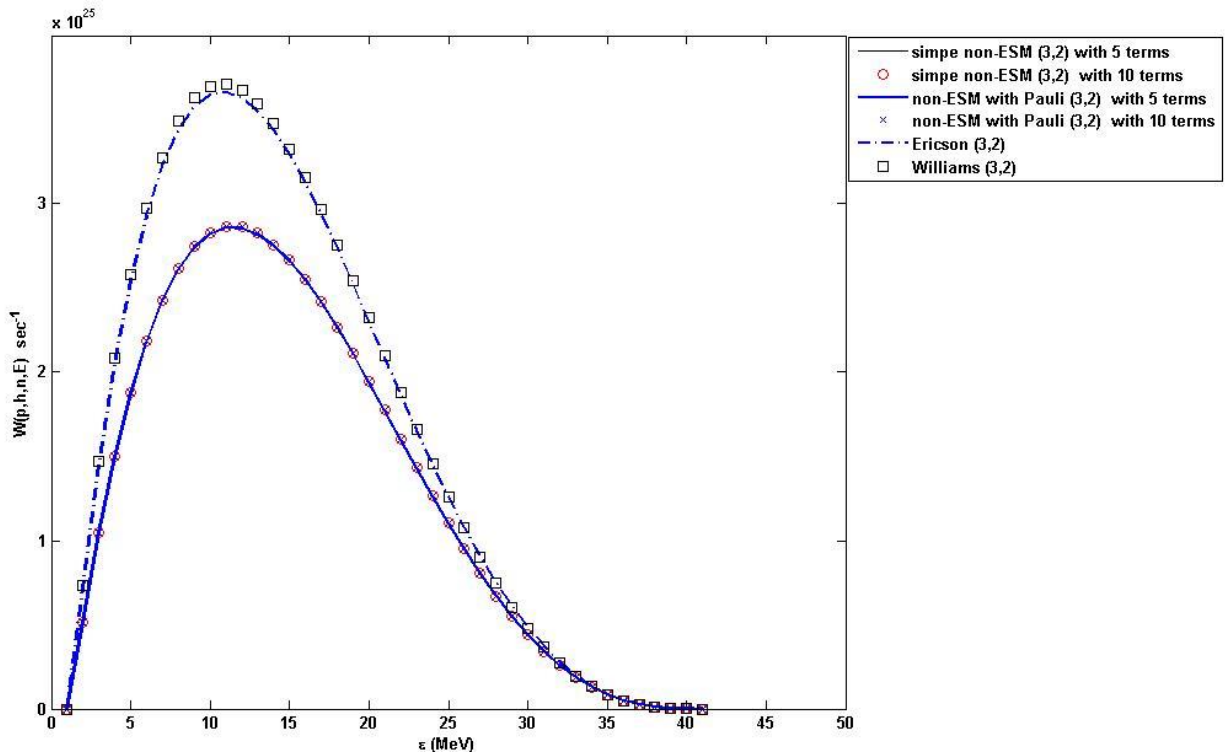


Figure (2-d). The same as Figure (2-b) for configuration (3,2).

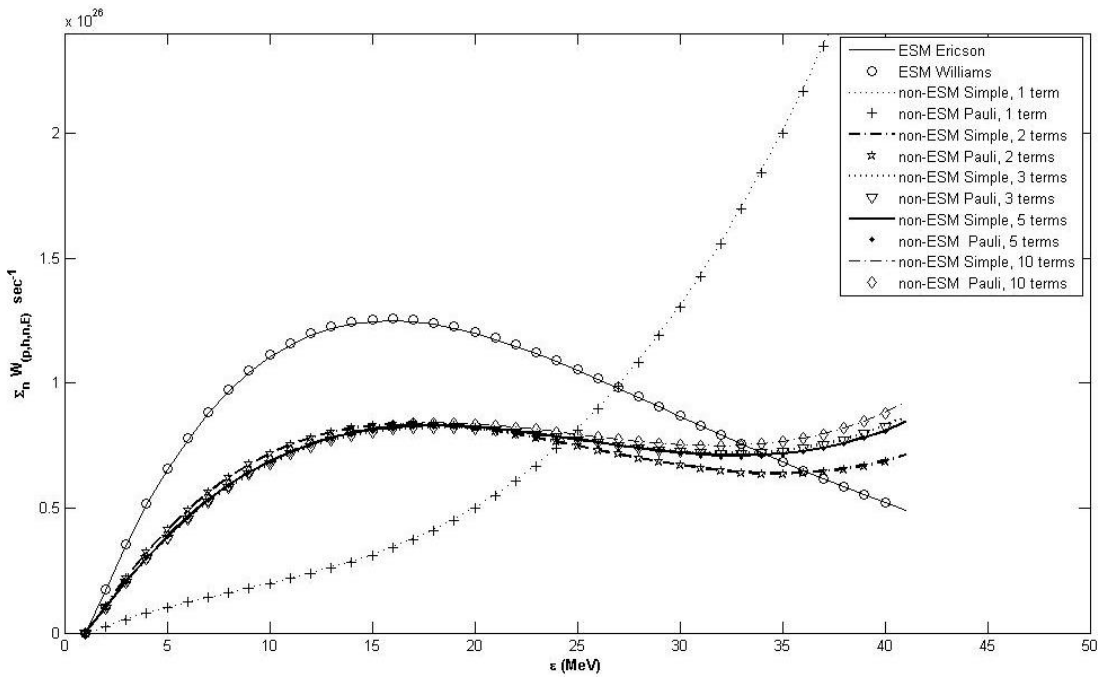


Figure (3). Comparison of the summation of emission rates from ESM and non-ESM systems with various summation terms. Bounded conditions are used.

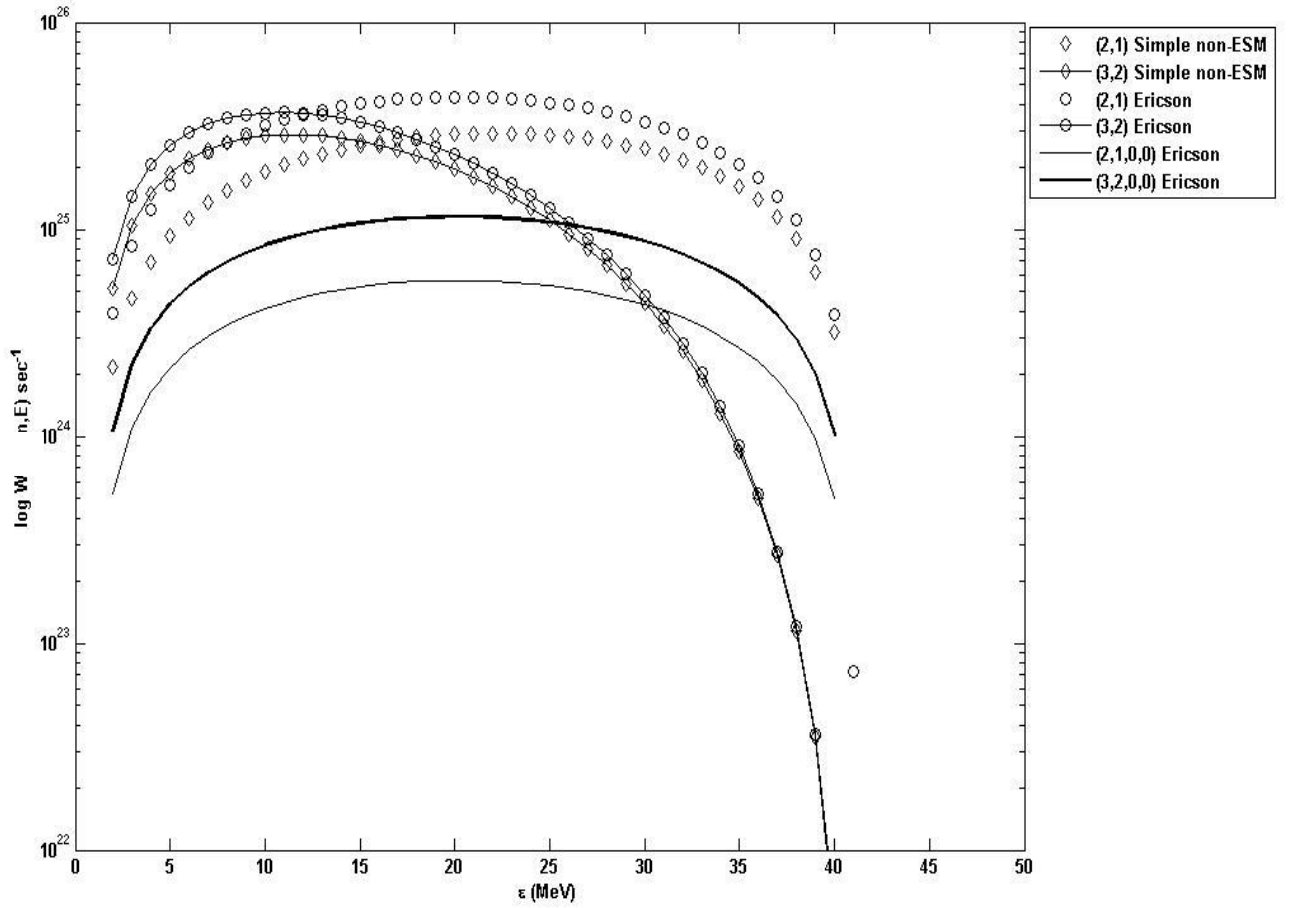


Figure (4). Comparison of the emission rates from ESM and non-ESM systems for one-component, with ESM for two-component for ⁹⁶Mo. Bounded conditions are used.

All ESM calculations indicated similar behavior, although same (total) exciton number is used (3 or 5 in this case), two-component showed less values. This was explained [20] due to the effects of sharing the excitation energy among more *types* of excitons, rather than *numbers*. Both non-ESM and ESM curves with (2,1) configuration contributed with higher emission rates at low energies yet dropped faster at higher energies, which will appear as a contribution in the low-energy evaporation (compound) region during cross-section calculations.

Conclusions

Emission rates have been numerically calculated for ^{96}Mo target with (N,N) reaction at 50 MeV. Both ESM and non-ESM simple formulae were used, and many comparisons were made. The final conclusions of this research are:

1. Earlier state density calculation did not reveal the weakness of the simple non-ESM formula when particle number is zero. This is attributed to the effect of Fermi energy on the state density calculation, for when $E > F$, some restrictions must be noted in the non-ESM application. This was obvious in the case of $(p, h) = (1, 1)$ configuration.
2. Both value and ratio between residual to initial state densities of non-ESM system are less than in the ESM. This may indicate the importance of the present non-ESM treatment in the exciton model calculation, although it is still an approximate one.
3. A general observation is seen that as the exciton configuration develops, the emission rates peaks to higher values at low energies and drop faster at higher energies. This case becomes more evident in the non-ESM system and it was explained due to the more corrected

energy-dependence of the s.p.l.d. of the system.

4. The important remark found is that, increasing the number of terms reduces the emission rates, for the same configuration when using the non-ESM rather than the ESM state density formulae.

5. Using 3 terms in the non-ESM might suffice to give correct treatment, but results indicated that changes continue to occur for five terms and even for ten terms, although with decreasing significance. Comparisons of accuracy with run time strongly favor the five terms calculation.

References

- [1] J. J. Griffi: Phys. Rev. Lett., 17(1966)478.
- [2] M. Blann: Ann. Rev. Nucl. Sci., 25(1975)123.
- [3] M. Blann: Phys. Rev. Lett., 18(1968)1357.
- [4] M. Blann: Phys. Rev. Lett., 27(1971)337.
- [5] M. Blann and M. B. Chadwick: Phys. Rev., C57(1998)233.
- [6] M. Blann: Phys. Rev., C57(1998)233.
- [7] J. Dobeš and E. Běták: Z. Phys., A310 (1983)329.
- [8] C. K. Cline and M. Blann: Nucl. Phys., A172(1971)225.
- [9] F.C. Williams: Nucl. Phys., A166(1971)231.
- [10] Y. C. Fu: Nucl. Sci. Eng., 86(1984)344.
- [11] C. Kalbach: Phys. Rev., C73(2006)024614.

- [12] C. Kalbach: Phys. Rev., C32(1985)1157
- [13] C. Kalbach: Phys. Rev., C33(1986)818.
- [14] C. Kalbach: Phys. Rev., C47(1993)587.
- [15] E. Běták and P. E. Hodgson, "Particle-Hole State Density in Pre-equilibrium Nuclear Reactions", University of Oxford, CERN Libraries, Geneva, OUNP-98-02 (1998).
- [16] M. Herman, G. Reffo, and C. Costa: Phys. Rev., C39 (1989) 1269.
- [17] M. Blann: Phys. Rev. Lett., 28(1972)757.
- [18] M. Avrigeanu and V. Avrigeanu: Comp. Phys. Comm., 112(1998)191.
- [19] A. Harangozo, I. Şteţcu, M. Avrigeanu and V. Avrigeanu: Phys. Rev., C 58(1998)295.
- [20] A. A. Selman: Ph.D. Thesis, University of Baghdad-College of Science, (2009).
- [21] T. Ericson: Adv. Phys. 9(1960)425.
- [22] Ye. A. Bogila, V. M. Kolomietz, and I. A. Sanzhur: Z. Phys. A, 341(1992)373.
- [23] C. Kalbach: "Users Manual for PRECO-2006", Triangle Universities Nuclear Lab., Duke University, (February 2007).
- [24] M. H. Jasim, S. Sh. Shafik, and A. A. Selman: J. Kerbala Uni., 7(2009) 271.
- [25] A. A. Selman, M. H. Jasim and S. S. Shafik: accepted for publication at the Iraqi Journal of Science, (December 2009).
- [26] A. A. Selman, EMNUR Matlab Code (unpublished,2010).